

Structure and magnetic properties of iron oxide dispersed silver based nanocluster composite

T. NAKAYAMA

The Institute of Scientific and Industrial Research, Osaka University, 8-1 Mihogaoka, Ibaraki, Osaka 567-0047, Japan

T. A. YAMAMOTO

Department of Nuclear Engineering, Osaka University, 2-1 Yamadaoka, Suita, Osaka 565-0781, Japan

Y.-H. CHOA, K. NIIHARA*

The Institute of Scientific and Industrial Research, Osaka University, 8-1 Mihogaoka, Ibaraki, Osaka 567-0047, Japan

E-mail: niihara@sanken.osaka-u.ac.jp

Magnetic nanocomposites composed of iron oxide and silver were fabricated by an inert gas condensation (IGC) method combined with co-evaporation, *in situ* oxidation, and *in situ* compaction techniques. The particle sizes of composite powder were controlled by varying helium gas pressure between 1 and 10 Torr, with the smallest one being about 10 nm at 1.0 Torr. The nanostructure of the composites was characterized by TEM. The magnetization behaviors were analyzed taking into account both the paramagnetic (PM) and ferromagnetic (FM) contributions to investigate the correlation between the nanostructure and the magnetic properties. It was found that some composites exhibit the superparamagnetism evidencing magnetically isolated grains as a single domain. TEM observation assisted with EDX revealed that iron nanocluster of a few nanometers size were surrounded by silver grains. Variation of the magnetic property of the nanocluster composites was also related to nanocluster size and heat treatment in an oxygen atmosphere. © 2000 Kluwer Academic Publishers

1. Introduction

In recent years, much attention has been paid to artificial engineered nanostructured magnetic materials because of their many attractive scientific aspects and technological applications such as giant magnetoresistance devices and advanced working substances for magnetic refrigeration [1]. Specially, the iron oxide dispersed metallic silver based nanocomposites have been studied because this system shows superparamagnetism due to isolated ferromagnetic iron oxide nanoparticles in the paramagnetic silver matrix [2, 3, 4]. We have found that iron oxide dispersed silver based nanocluster composites could be synthesized by inert gas condensation (IGC) method to obtain the bulky materials and briefly reported that this composite materials shows the superparamagnetism and the heat treatment in O₂ atmosphere modifies magnetic properties [2]. These studies indicated that the IGC process could be a potential synthesis route for magnetic nanocluster composites useful for the suggested applications. In these studies, however, the correlation between particle size of iron oxide and magnetic properties, which is closely related to nanostructure, has been not clearly investigated. There-

fore, the objective of this study is to fabricate iron oxide dispersed silver based nanocluster composites with various particle sizes of the iron oxide and is to evaluate the relationship between the particle size of the iron oxide and magnetic properties. In addition, oxidation effects at high temperature on the magnetic properties and morphology of the iron oxide were investigated for iron oxide dispersed silver based nanocluster composites.

2. Experimental procedure

Iron oxide dispersed metallic silver based nanocluster composites were synthesized by the IGC method combined with a co-evaporation process [2]. Metallic iron and silver were used as source materials, and these metals were evaporated by resistance heated boats in a chamber filled with helium gas. The particle size of the metallic iron and silver mixture is controlled by the inert helium gas pressure of 1 to 10 Torr. The helium gas quenches the metallic vapor, and nanoparticles are formed above the boats and transported to the surface of a particle collector cooled by liquid nitrogen. The collector is cylindrical and rotates during the evaporation

* Author to whom all correspondence should be addressed.

process to obtain a homogeneous mixture of the two phases. After evaporation, only the iron particles are oxidized by oxygen gas exposure up to 1.0 Torr. Subsequently, the silver and iron oxide powder mixture is scraped off the collector surface and transported *in situ* to a chamber for compaction. The compaction condition is 400 MPa at room temperature. From these samples, one was post-annealed in an oxidizing atmosphere of 10% O_2/Ar at 473 K for 1 h to investigate the oxidation effect on the phase transformation of iron and iron oxide. The microstructures of the nanocluster composites were studied by high resolution TEM (HRTEM) with an energy dispersive X-ray spectrometer (EDX). The composition of the each composite mixture was measured by EDX analysis and X-ray near edge absorption spectroscopy (XANES). Magnetization were measured by a SQUID magnetometer with a maximum field of 5 Tesla at 100, 150, 200, 250 and 300 K.

3. Results and discussion

The particle size of the composite mixture is controlled by the inert helium gas pressure from 1 to 10 Torr, and increased with an increase of helium gas pressure for the loose composite powder. Fig. 1a and b show TEM micrographs of the loose composite powder obtained at helium gas pressures of 1.0 and 10 Torr, respectively. The average particle size of the composite mixture was 12 nm at 1.0 Torr, and 26 nm at 10 Torr. The nucleation and growth of iron and Ag was closely related to the concentration of inert helium gas, and readily took place as a result of by the higher frequency of collision between vapor atoms at a higher helium gas pressure. Therefore, it is believed that the higher helium gas pressure induced the larger particle size. In addition, a specific microstructure feature for the nanocluster composite prepared at a helium gas pressure of 1.0 Torr was obtained as shown in Fig. 2. Fig. 2 shows the high magnification TEM micrograph of the loose nanocluster composite powder obtained at a helium gas pressure of 1.0 Torr, corresponding to Fig. 1a. Intragranular iron nanocluster of 2–3 nm was observed within the silver matrix particles and intergranular particles of 12 nm the same size as the silver matrix particles. This observation was attributed to the helium gas pressure. At a high helium gas pressure, each iron and silver vaporised atom rapidly and independently first formed nuclei of its the each other, and these nuclei were grown up. However, at a low helium gas pressure, iron vapor formed the nuclei because of high evaporation rate [5], and subsequently, this iron nucleolus acted as a substrate for heterogeneous nucleation of silver. Therefore, it is believed that intragranular iron particles existed within the silver particles. An EDX analysis with an electron beam focused on a region of 20 nm indicated that the components of the grains consisted of silver and iron, as shown in Fig. 2, which showed that iron particles of a few nanometers were surrounded by silver grains during the evaporating. However, some large intergranular iron oxide particles are also observed with intragranular particles due to agglomeration.

The composition of the each composite mixture was measured by EDX analysis and X-ray near edge absorp-

tion spectroscopy (XANES) for as compacted composites and oxidized composites at 473 K. For XANES measurements, the composition of the composite powder was calculated from linear combination Fe-K near edge spectra and reference iron oxide spectra as in ref. [4]. From these measurements, the composite loose powder contained 20 at.% iron, and the ratio of iron, $\gamma\text{-Fe}_2\text{O}_3$ and Fe_3O_4 was 46.5 at.%, 25 at.%, and 23.5 at.% for a composite powder prepared at 1 Torr, and was 25 at.%, 45 at.%, and 30 at.% respectively for a composite powder prepared at 10 Torr. The remaining metallic iron was completely oxidized to $\gamma\text{-Fe}_2\text{O}_3$ by the heat treatment in oxygen atmosphere at 473 K, and silver was found to exist as a stable metal by X-ray diffraction up to 473 K. Furthermore, it was observed that the composites with particle sizes 12 nm and 26 nm prepared at 1.0 Torr and 10 Torr increased to 20 nm and 30 nm by heat treatment in an oxygen atmosphere at 473 K, respectively.

The magnetization (emu/g) estimated from the data of iron concentrations from EDX and XANES measurements was plotted against H/T for the nanocluster composite as compacted powder obtained at helium pressure of (a) 1.0 and (b) 10 Torr in Fig. 3. The data all points of samples lie on a single curve, providing evidence for the occurrence of superparamagnetism [2, 3]. The as-compact sample prepared at a helium pressure of 1.0 Torr (denoted by ACS) showed superparamagnetic behavior down to 100 K, while the as-compact sample prepared at a helium pressure of 10 Torr (denoted by ACL) showed this down to 150 K. This result is attributed to the difference in particle size between the ACS and ACL samples observed by TEM, as shown in Fig. 1, because the superparamagnetism of the sample with a smaller particle size persisted to a lower temperature.

To investigate the magnetic properties in detail, the magnetization curves, $M_{\text{Total}}(H)$, were separated into a ferromagnetic (denoted by FM) and a superparamagnetic (denoted by SP) part by following the formula [6].

$$M_{\text{Total}}(H) = \frac{2M_{\text{FM}}^S}{\pi} \tan^{-1} \left[\frac{H \pm H_C}{H_C} \tan \left(\frac{\pi S}{2} \right) \right] + N_g \mu \left[\coth \left(\frac{\mu H}{kT} \right) - \left(\frac{\mu H}{kT} \right)^{-1} \right]$$

The first term is a function to represent a FM hysteresis curve and the second is the Langevin function to express the SP component. M_{FM}^S and $N_g \mu (=M_{\text{SP}}^S)$ are saturation magnetizations corresponding to the FM and SP parts, respectively. S is a parameter of the squareness of the FM loop, i.e., the ratio of the remanent magnetization, M_R , to M_{FM}^S . The average size of magnetic moment giving rise to SP, μ , and number of the moments, N_g , in the SP fraction are obtained from the second term. Typical fits to the magnetization curves are shown in Fig. 4 for the ACS and ACL. From this fitting, the SP fraction $M_{\text{SP}}^S/M_{\text{Total}}^S$ was calculated for various temperatures as shown in Fig. 5. In the same manner, the SP fraction, $M_{\text{SP}}^S/M_{\text{Total}}^S$, was also obtained

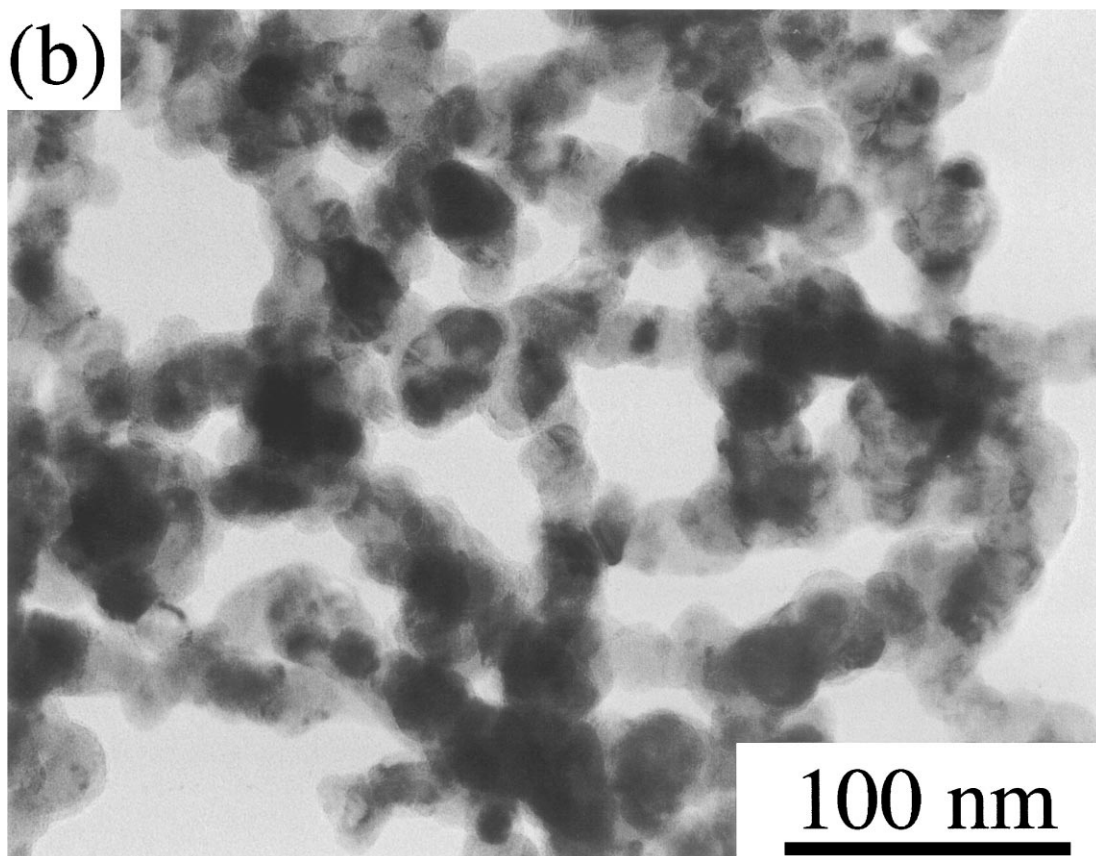
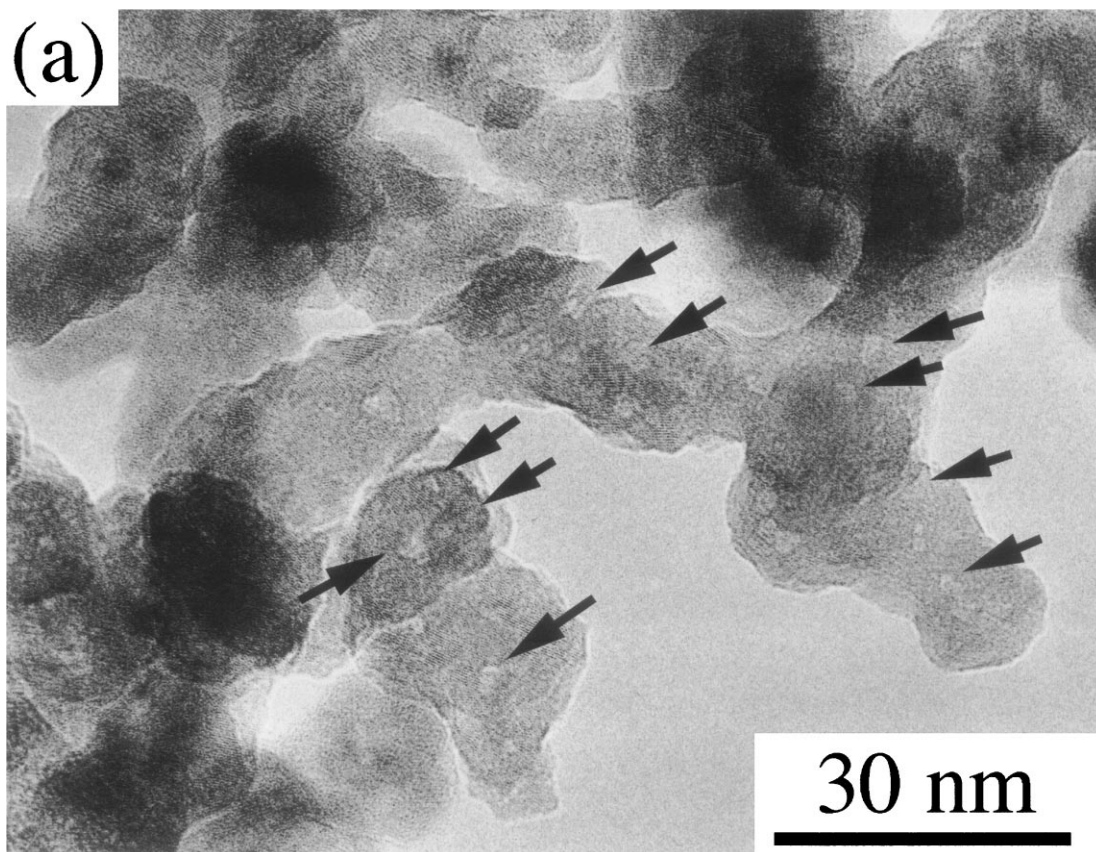


Figure 1 TEM micrographs of the nanocomposite loose powder obtained at helium pressures of (a) 1.0 and (b) 10 Torr.

for heat treated ACS and ACL in an oxygen atmosphere at 473 K (denoted by OACS and OACL, respectively). From this approach, several features were observed; i) the SP fraction M_{SP}^S/M_{Total}^S significantly increased with increasing temperature for ACS and OACS, and

the change of fraction for ACL and OACL with temperature was not significant compared with that for ACS and OACS, ii) the fraction for ACS is higher than that for ACL, and iii) the fraction for OACS and OACL is higher than that for ACS and ACL.

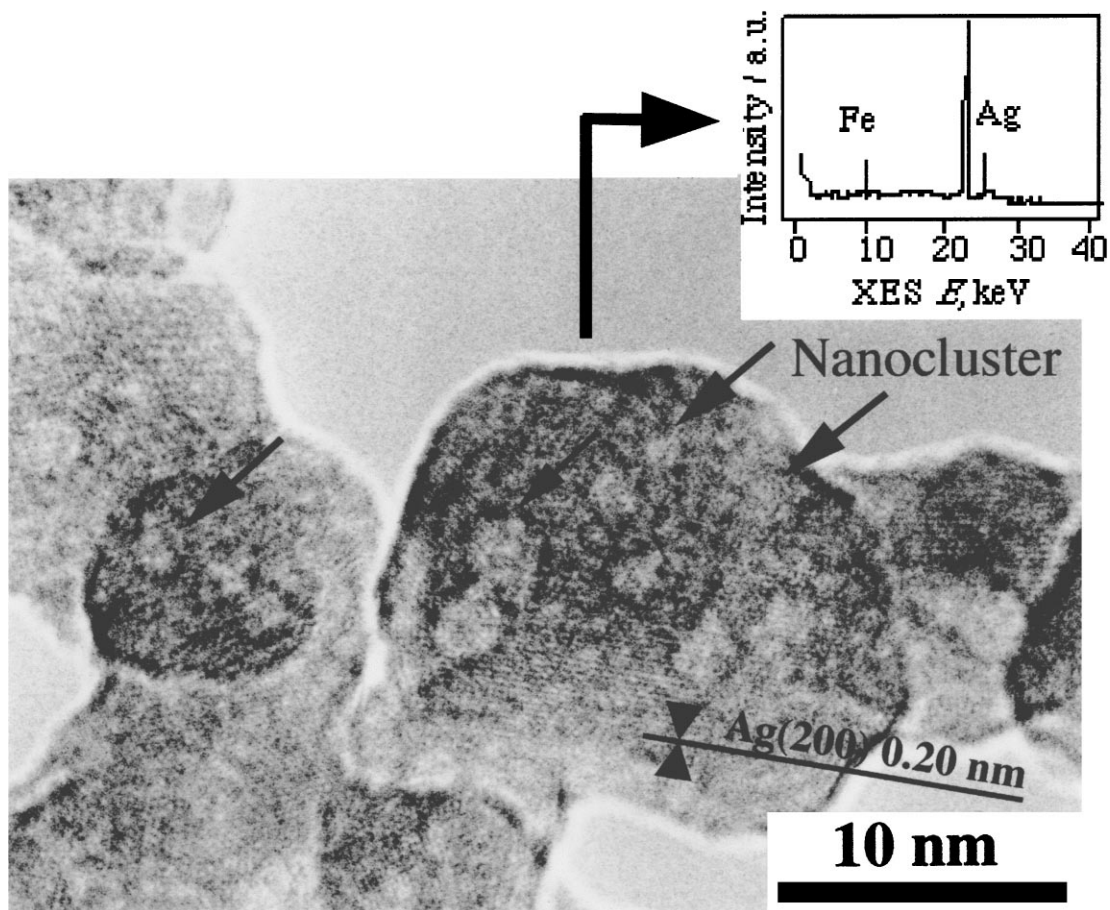


Figure 2 High magnification TEM micrograph and EDX spectrum (inset) of the nanocomposite loose powder obtained at a helium pressure of 1.0 Torr, corresponding to Fig. 1a.

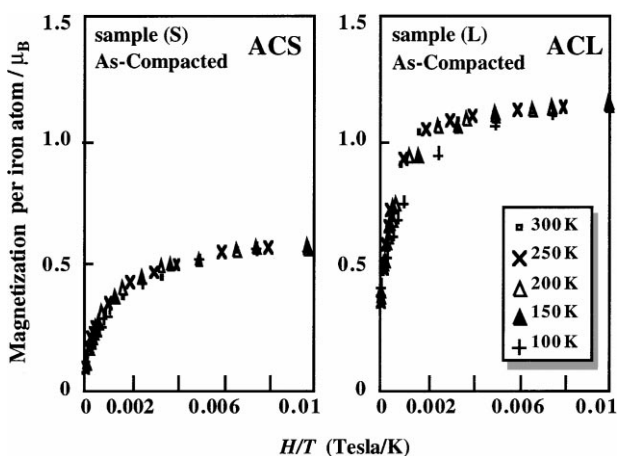


Figure 3 Plots indicate superparamagnetism occurrence in the ACS and ACL.

For these observations, the following deductions can be made. Firstly, at higher temperature, the spin direction for magnetic nanoparticles was flipped by the higher thermal energy compared to the magnetic interaction energy and anisotropy energy. Therefore, the SP fraction increased with increasing temperature for ACL and OACL. On the other hand, the change of fraction for ACL and OACL with temperature was not significant compared with ACS and OACS with a lower SP fraction. This is attributed to the larger particle size of ACL and OACL compared with ACS and OACS, because the larger one is relatively insensitive to temperature.

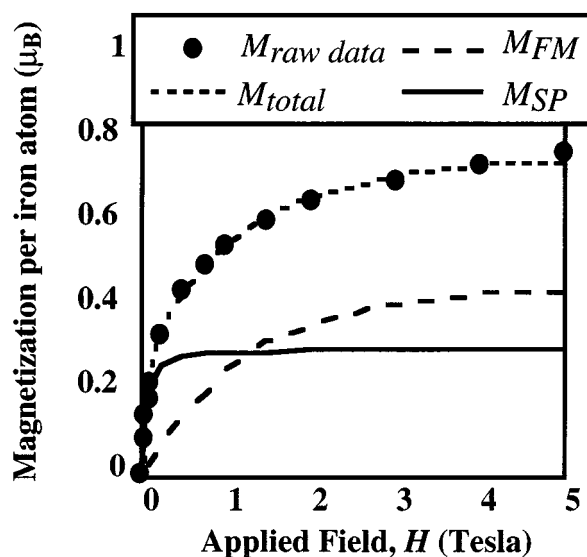


Figure 4 Deconvolution of the measured total magnetization curves into their ferromagnetic and superparamagnetic components for the ACS.

Secondly, the reason for the higher SP fraction for ACS with an even higher iron content (46.5 at.%) than that for ACL was closely related to the microstructure of each sample. In general, a higher iron content induced a smaller SP fraction due to a higher crystalline anisotropy energy and saturation magnetization for the same particle size compared with other components (Fe_3O_4 and $\gamma\text{-Fe}_2\text{O}_3$) in the present composite systems, as discussed below. However, a different

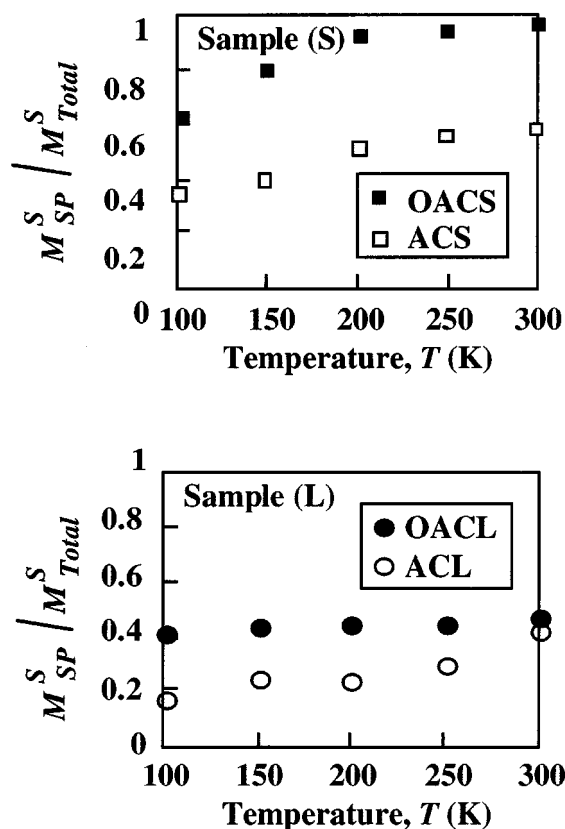


Figure 5 Variation of the superparamagnetic fraction of the total moment, M_{SP}^S / M_{Total}^S .

feature was observed for ACS. This could be caused by the intragranular iron nanoparticle of 2–3 nm within the silver matrix particle, as shown in Fig. 1. When the iron particle size is 2–3 nm, the iron also shows the superparamagnetism, as a result, it is believed that the SP fraction for ACS is higher than for ACL.

Finally, the reason for observing a higher SP fraction by oxidization was a phase transformation of metallic iron to γ -Fe₂O₃. A γ -Fe₂O₃ phase is more easily in a superparamagnetic state than a metallic iron phase for the same particle size. The critical particle size to be in a superparamagnetic state for γ -Fe₂O₃ is larger than that for metallic iron at the same temperature, because the crystalline anisotropy energy (K_1) and saturation magnetization (σ_s) of γ -Fe₂O₃ are significantly lower than those of metallic iron. K_1 (ergs/cm³) and σ_s (emu/g) are -0.46 (at room temperature) and 73.5

(at room temperature) for γ -Fe₂O₃ and 5.7 (at 77 K) and 217.2 (at room temperature) [7] for metallic iron, respectively. Therefore, it is believed that a higher SP fraction on oxidization was observed, even though the particle size was increased to 20 nm and 30 nm for OACS and OACL as discussed earlier.

4. Conclusion

The nanostructure of the iron oxide dispersed silver based nanocluster composites was investigated by TEM and magnetic properties measured by a SQUID magnetometer. Nanocluster composites with various particle sizes of iron oxide were fabricated by controlling the helium gas pressure from 1 to 10 Torr. The particle size of the composites increased with increasing helium gas pressure for loose composite powder. For the composite powder prepared at 1.0 Torr, a specific microstructure with intragranular iron nanoclusters of 2–3 nm within the silver matrix particles with a size of 12 nm was observed, this microstructure affects the superparamagnetic property. To investigate the magnetic properties in detail, the magnetization curves, $M_{Total}(H)$, were separated into a ferromagnetic and a superparamagnetic part. Oxidation of the loose powder induced the phase transformation of iron to γ -Fe₂O₃, and increased the superparamagnetism fraction.

References

1. R. D. SHULL, L. J. SWARTZENDRUBER and L. H. BENNET, in Proceedings of the 6th International Cryocoolers Conference, Annapolis, April 1991, edited by G. Green and M. Knox (David Taylor Research Center Publication, 1991) p. 231.
2. T. A. YAMAMOTO, R. D. SHULL, P. R. BANDARU, F. COSANDEY and H. W. HAHN, *Jpn. J. Appl. Phys.* **33** (1994) L1301.
3. T. NAKAYAMA, T. A. YAMAMOTO, Y. H. CHOA and K. NIIHARA, *Key Engineering Materials* **161–163** (1999) 497.
4. H. W. HAHN, J. A. EASTMAN and R. W. SIEGEL, *Ceramic Transactions* **1b** (1988) 1115.
5. T. A. YAMAMOTO, M. C. CROFT, R. D. SHULL and H. W. HAHN, *Nano Structured Materials* **6** (1995) 965.
6. M. B. STEARNS and Y. CHENG, *J. Appl. Phys.* **75** (1994) 6894.
7. R. M. BOZORTH, *ibid.* **39** (1968) 504.

Received 3 June 1999

and accepted 3 February 2000